Published in final edited form as:
J Neurosci Methods. 2014 January 15; 221: . doi:10.1016/j.jneumeth.2013.10.004.

Novel test of motor and other dysfunctions in mouse neurological disease models

Albert M.I. Barth, PhD[a] and **Istvan Mody, PhD**[a,b]

[a]Department of Neurology, The David Geffen School of Medicine at the University of California, Los Angeles, CA 90095, USA

[b]Department of Physiology, The David Geffen School of Medicine at the University of California, Los Angeles, CA 90095, USA

Abstract

Background—Just like human neurological disorders, corresponding mouse models present multiple deficiencies. Estimating disease progression or potential treatment effectiveness in such models necessitates the use of time consuming and multiple tests usually requiring a large number of scarcely available genetically modified animals.

New method—Here we present a novel and simple single camera arrangement and analysis software for detailed motor function evaluation in mice walking on a wire mesh that provides complex 3D information (instantaneous position, speed, distance traveled, foot fault depth, duration, location, relationship to speed of movement, etc.).

Results—We investigated 3 groups of mice with various neurological deficits: 1) unilateral motor cortical stroke; 2) effects of moderate ethanol doses; and 3) aging (96–99 weeks old). We show that post stroke recovery can be divided into separate stages based on strikingly different characteristics of motor function deficits, some resembling the human motor neglect syndrome. Mice treated with moderate dose of alcohol and aged mice showed specific motor and exploratory deficits.

Comparison with Existing Methods—Other tests rely either partially or entirely on manual video analysis introducing a significant subjective component into the analysis, and analyze a single aspect of motor function.

Conclusions—Our novel experimental approach provides qualitatively new, complex information about motor impairments and locomotor/exploratory activity. It should be useful for the detailed characterization of a broad range of human neurological disease models in mice, and for the more accurate assessment of disease progression or treatment effectiveness.

Keywords

stroke; video; motor performance; wire mesh; open field; hole board

Corresponding author: Istvan Mody, Ph.D., Corresponding author's address: Department of Neurology, NRB1 Room 575D, 635 Charles E. Young Dr. S., Los Angeles, CA 90095, USA, Corresponding author's phone and fax: 310 206-4481; 310 825-0033, Corresponding author's email address: mody@ucla.edu.

1. Introduction

Over the past decades the increasing number of human disease models in mice has lead to an increased necessity of the detailed behavioral characterization of these animals. Several tests for motor function originally developed for rats have been adapted for mice, but presently only the gait analysis, rotarod test and the parallel rod floor test are fully automated (Rozas, Guerra et al., 1997;Kamens and Crabbe, 2007;Brooks and Dunnett, 2009). Other tests rely either partially or entirely on manual video analysis (Brooks and Dunnett, 2009). This introduces a significant subjective component into the analysis, and fails to account for several detailed but measurable parameters which may be important for data interpretation (e.g., running speed on a grid). Moreover, to provide a net motor deficit, the vast majority of the currently measured tasks rely on assessing binary events (e.g., fault/no fault, fall/no fall). Even the automated parallel rod floor test provides only binary information, i.e., did faults occur or not? (Kamens and Crabbe, 2007). Such quantitative measures, i.e., the number of times an event occurred, provide no information about qualitative parameters (e.g., what type of events occurred). Such lack of qualitative differences can result in animals showing similar performances in a given motor task in spite of motor deficits of different types or origins. To overcome the binary quantification more complex analyses such as the ladder rung walking test (Metz and Whishaw, 2002;Metz and Whishaw, 2009) have been developed. In this test, different types of motor faults can be separated, but the results are still entirely based on time consuming and subjective manual video analysis. Other drawbacks of many currently available motor performance tasks include forcing the animals to move either by the experimenter if the animal stops (e.g., balance beam) or by the experimental conditions (e.g., rotarod) (Dunham and Miya, 1957;Brooks and Dunnett, 2009;Schaar, Brenneman et al., 2010). Such forced movement can interfere with the animal's natural motor performance by altering the anxiety level of the animal. These and other flaws of mouse motor performance tests together with the abundance of sophisticated mouse models of disease involving motor deficits point to the urgent need to develop computer-based complex approaches capable of providing qualitatively more detailed analyses.

Presently available computer-based behavioral analyses mostly use a single camera providing side or top view and the two-dimensional (2D) information derived from this type of recording. The major limitation of this approach is the loss of three-dimensional (3D) data which are necessary to analyze more complex movements, postures or motion components in different dimensions (i.e., horizontal animal movement with vertical limb faults). Using multiple cameras may overcome the 2D limitations (Oota, Mekada et al., 2009), but synchronization of 2 or more cameras and the combined video analysis requires special equipment and increasingly more complicated analysis software that is presently unavailable for the broad research community. Here we present a novel and simple single camera arrangement and the corresponding analysis software for detailed motor function evaluation in mice walking on a wire mesh. Our approach provides qualitatively more 3D information (instantaneous position, speed, traveled distance, location preference, foot fault depth, duration, location, relationship to speed of movement, etc.). The arrangement of the camera shown here may be implemented for recording other motor tasks (e.g., parallel rod floor test) or for other types of computer based behavioral analyses where 3D observations are required (e.g., pathological postures).

We tested the analysis in three groups of mice with motor impairments: 1) one day to eight weeks following unilateral photothrombotic stroke to the forelimb motor cortex, 2) moderate dose ethanol treated and 3) aged (>96 week old) animals. We found different limb fault parameters, locomotor and exploratory activities in the three groups. We also show that over

8 weeks of recovery period following stroke, robust differences are present in the temporal evolution of the various types of foot faults.

2. Material and methods

For the experimental setup and description of the calculations made by the software please refer to the Supplementary Methods section. This study used C57BL/6 mice housed with *ad libitum* access to food and water under the care of the UCLA Division of Laboratory Animal Medicine (DLAM). Mice were maintained on a light/dark cycle of 12 hours, and all experiments were performed during the light period. All experiments were performed according to a protocol (ARC # 1995-045-53B) approved by the UCLA Chancellor's Animal Research Committee.

2.1. Surgery for stroke induction

Surgeries were performed under aseptic conditions on male mice weighing 25–30 g (2–3 months of age). Under isoflurane anesthesia (2–2.5% in O_2 alone) the animal was mounted into a standard Stoelting instrument stereotaxic frame with blunt ear bars. Body temperature was maintained at 37°C using a rectal probe and a water circulated heating pad. The cranium was exposed through a small midline scalp incision. The bone was dried and a short thin wall tube covered by thin parafilm (3 mm outer diameter) was placed above the future stroke area (centered at AP: 0 mm; ML: 1.5 mm). The tips of the head holder for the spherical treadmill, covered by thin parafilm were positioned above the caudal part of the skull bilaterally then cranioplastic cement was used to embed the tips of the head holder and the small tube. After the dental cement hardened the head holder and the small tube were removed leaving slots bilaterally in the implant and a clean skull surface spared from the dental cement above the intended stroke area.

Immediately after surgery, the mouse was continuously monitored until recovered, as demonstrated by their ability to maintain sternal recumbency and to exhibit purposeful movement. During the recovery period after surgery, warm saline solution (0.01–0.02 ml/g/twice/day) was administered subcutaneously to prevent dehydration. To prevent any infection around the implant we topically administered Neosporin for 7 days.

2.2. Stroke induction

After 7–10 days postsurgical recovery the mouse was placed on the top of an air supported polystyrene ball. To record ball rotation produced by running and walking, two optical computer mice were positioned close to the ball along the equator at 90° apart (Dombeck, Khabbaz et al., 2007;Harvey, Collman et al., 2009). After the animal was allowed to habituate to the setup for 5 min an injection of 10 mg/ml solution of Rose Bengal (100 mg/kg, i.p.) in physiological saline (10 mg/ml) was administered. To induce cortical ischemia a 532 nm diode laser was positioned above the portion of the skull not covered by dental cement. To photoactivate the Rose Bengal, the targeted cortical area was illuminated (70 mW for 7 min) through the intact skull using an aspheric lens (Thorlabs) giving a 2 mm diameter illumination area. Using this procedure we were able to induce targeted cortical ischemia in awake moving animals avoiding the compromising effects of anesthetics on the stroke pathogenesis. The photothrombosis targeted the same brain area as in our previous collaborative work (Clarkson, Huang et al., 2010). Based on published data this region predominantly contains the forelimb motor area but also comprises small segments of the hindlimb motor area (Clarkson, Huang et al., 2010;Clarkson, Lopez-Valdes et al., 2013). Sham control animals were injected i.p. with the same volume physiological saline solution and were illuminated using the same laser parameters as the stroke induced animals.

2.3. Navigation on air supported ball

Beyond the automated grid walking analysis we tested the animals following stroke for potential movement impairments on an air supported spherical treadmill. The forward-backward and sideways movement of the spherical treadmill was tracked using two optical computer mice positioned at 90° (Dombeck, Khabbaz et al., 2007; Harvey, Collman et al., 2009). The animal's movements were recorded at different timepoints before and after the stroke induction (Days: −5, −3, 1, 2, 3, 7, 14, 21, 28, 35, 42, 56). To avoid the necessity for repeated transient anesthesia before attaching the head implant to the holder we developed a novel technique which simply and quickly attaches the head implant to the holder and avoids the need to cement a head bar to the skull. We designed a holder similar to a long-nose forceps with its tips bent towards each other. These pyramidal shaped tips could be hooked into the preformed slots (see surgery details) on both sides of the implants. The pyramidal shape of the tips and the force pushing the tips toward each other ensured the secure holding of the mouse head through the implant.

2.4. Statistical analyses

Statistical analyses were performed using Igor Pro 6.30 (Wavemetrics, Lake Oswego, OR) or Microsoft Office Excel. We used two-tailed pairwise t-test for numerical comparisons across different conditions for the same dataset. For comparison of different datasets two-tailed unpaired t-test was used (significance level <0.05). Summary reports of data are presented as arithmetic means together with the standard error of the mean (SEM). Data normality was verified using Shapiro-Wilk test (with $p<0.05$ significance level).

3. Results

3.1. Automated tracking of motor performance

We developed a novel experimental setup to obtain 3D information using only one camera. Two side mirrors were used along the shorter and longer side of a transparent cage with wire mesh bottom. A top mounted camera captured the movement of the animal on the wire mesh occupied in the central part of the image, while the two mirrored side-view images were projected on the two sides of the video image (Supplementary Fig 1). The central image provided information about the animal's speed, location and orientation; the mirrored images were used to detect the movement of a specific body part through the grid, i.e., depth, duration and 1 dimensional side projected location. We developed a program in Igor Pro 6.30 (Wavemetrics, Lake Oswego, OR) to analyze the video recordings. The combination of the three image segments yielded the 3D data necessary to determine the exact body part (snout/head, tail or limbs) protruding through the grid, hereafter referred to as a "fault". The software also correctly reconstructed several characteristics of the real 3D faults (Supplementary Videos 1 and 2). Multiple parameters could thus be derived based on the 3D information (Fig 1): total distance, average speed, time-instantaneous speed, fault-speed relation, animal location trajectory, center-peripheral location preferences, fault locations on the grid, normalized relative fault location to the body part, fault duration-depth matrices for each limb, distribution of the fault depth and fault durations for each limb, head and tail, grouping the faults based on their depth and duration, animal rotations, etc. The experimental arrangement described here solved the problem of how to record all the required 3D information with a single camera (for further details refer to Online Methods).

3.2. Validation of the software measurements

During the computerized "fault" detection we chose the threshold level to avoid only the shallowest events (i.e. when the animal normally grabs the wire and only the fingers/toes appear below the grid). We hypothesized that any event deeper than this threshold can be a sign of potential pathologically relevant performance. Our approach therefore was not an "a

priori" definition of the faults but rather the detection of all events deeper than the basic threshold (avoiding detection of only fingers/toes under the grid), followed by categorization based on different parameters (duration and depth). Comparing each of the fault categories with those in control animals while taking into account other parameters (i.e. open field) will tell whether certain events clearly deviate from the normal or they can be explained by an indirect effect (i.e. faster running may cause more faults).

To validate the setup and the software, video recordings of four mice were visually analyzed frame-by-frame by 2 independent human observers in a blind manner counting the faults made by each limb.

Because of the above mentioned software's thresholding approach, the observers were asked to count the less obvious shallower faults as well. This explains the relatively lower agreement between the observers (on the 4 videos analyzed, 63–73 % of the faults were recognized by both observers), the less characteristics shallow faults result in larger variations between subjective manual analyses. However, overall the manual and the computerized analyses provided similar event numbers (Supplementary Fig 2).

3.3. Recovery of motor function after photothrombotic stroke to the forelimb motor cortex

To test the sensitivity of our system for functional recovery after stroke, we induced stroke in 4 animals in the forelimb motor cortex using a modified version of the photothrombotic method. We tested the animals at different time points before and after the stroke induction for up to 8 weeks. At every time point 10 min long video recordings were analyzed. Sham control animals were injected i.p. with the same volume physiological saline solution and were illuminated using the same laser parameters as the stroke group. The sham control fault numbers were calculated as the average of the two sides. The software was able to detect differences in the fault numbers between the affected and non affected limbs in all animals and during the entire investigated period (up to 8 weeks) (Fig 2, and Supplementary Table 1). Because the software recorded qualitatively more data than a manual video analysis, we were able to further refine the analysis of foot faults during the functional recovery period. In each 10 minute long video recording the faults were separated based on the limbs generating the faults.

Then for each limb a two-dimensional duration – depth histogram was created normalized to the distance covered. In this histogram a certain cell shows how many faults (normalized to the total distance walked) appeared on that limb with certain duration and fault depth. These duration-depth matrices were plotted at various times before and after stroke induction (Fig 2B,D). For statistical calculations we grouped the faults into 4 categories whether they were shallower/deeper or longer/shorter than a certain depth/duration threshold (short: <100 ms; long: >100 ms; shallow: <10 pixels; deep: >10 pixels). The values of the 4 categories were plotted at different timepoints (Fig 2A,C). The resulting plots showed qualitative differences in the temporal evolution of the different type of foot faults (Fig 2A). The long-deep events showed a transient peak just after stroke induction, then within 1–2 weeks rapidly returned to baseline. The short-deep events showed a similar rapid peak after stroke, and one week later they moderately decreased to a level that was still higher than the baseline. The shallow foot faults showed a highly different temporal evolution: they increased during the first week and remained elevated for the entire duration of the recovery period (up to 8 weeks). These results indicate that the separation of the foot faults into different categories may highlight important aspects of motor function recovery in mice. The various faults are differently affected by a stroke to the motor cortex and may be correlated with different patterns of functional recovery. The observed transient long-deep faults might indicate the appearance of compensatory mechanisms. Importantly, the findings also demonstrate that the computer-based approach can provide qualitative data over and beyond the currently

used manual video analysis, and these detailed data may reveal previously unattainable aspects of motor function in mice.

We also investigated open field parameters (traveled distance, average speed) and head dips before and after stroke induction but found no significant differences (data not shown).

3.4. Ethanol treated mice

We chose ethanol treated mice to test our setup because ethanol has multiple effects on motor performance including effects on movement coordination, locomotor and exploratory activities (Crabbe, Cameron et al., 2008). Therefore, ethanol treated animals are good subjects to test how our method is able to dissect different aspects of the motor performance.

The cerebellum plays a major role in balance, posture control and in coordinating sequences of movements (Morton and Bastian, 2004). Alcohol-induced alterations of cerebellar function cause motor coordination impairments (Valenzuela, Lindquist et al., 2010). The grid walking test was originally developed to investigate ethanol induced behavioral impairment in mice (Belknap, 1975). We tested our experimental arrangement by examining the motor function in moderate dose ethanol injected mice. Eight mice were injected with ethanol (i.p. 1.6 g/kg in 20 ml/kg physiological saline), and another 8 mice (sham controls) were injected with the same volume vehicle. Ten minutes after the injections mice were placed on the wire mesh and their activities were recorded for 10 min.

Ethanol-treated mice showed a robust increase in the number of faults on all four limbs when compared to sham control animals. The difference was most prominent in the number of deep faults (Fig 3).

Mice also tend to explore holes or openings in the substrate of their environment by stereotypically dipping their heads in and out of the opening. This is the basic concept of the “hole board test” that is widely used for measuring exploratory activity (Boissier, Simon et al., 1964). Because our setup also provides information similar to an open field and to a hole board test, we extended our analyses by measuring speed-distance and head dip parameters. We compared the total traveled distance, average speed, the fraction of the time spent moving and the center - periphery open field preference ratio but we did not find any significant differences between moderate dose ethanol-treated and sham control animals (Fig 4A to D). However, the number and total duration of head dips showed a robust decrease in the ethanol treated mice (Fig 4E to F). These results are agreement with earlier data showing that ethanol differently affects locomotor and exploratory activities and therefore they should be distinguished (Lister, 1987;Crabbe, Gallaher et al., 1994). Our findings also demonstrate how the novel experimental arrangement and software can simultaneously resolve different parameters of motor performance and exploratory behavior.

3.5. Aged mice

Motor performance decreases from young adulthood to old age in humans (Leversen, Haga et al., 2012) and also in mice (Anderson, Shanmuganayagam et al., 2009). It is known that age-related cerebellar alterations are crucially involved in the loss of fine motor control and balance (Forster, Dubey et al., 1996). To investigate the decline in the motor performance of aged mice we tested 6 old (96–99 weeks old) mice and compared their performance to 6 young adult mice (8–12 weeks old). The analysis revealed a prominent increase in the normalized number of shallow faults and also a significant increase in the normalized number of long-deep faults of the hind limbs (Fig 5).

The open field parameters showed a marked decrease indicating the declining locomotor activity in aged mice (Fig 6A to D). The number of head dips was also reduced in the old

animals (Fig 6E to F) in agreement with previously published findings on exploratory activity (Foreman, Lionikas et al., 2009).

4. Discussion

Here we have demonstrated a novel and simple recording method and the corresponding analysis software which combines multiple motor tests (open field, grid walking test, hole board test) and provides measures for multiple parameters of the motor behavior in mice. Our approach not only fills a gap in the field of mouse motor behavior but also demonstrates a simple way of how 3D information can be presented, recorded, and analyzed using a single camera. This idea can be applied to other fields in computer based behavioral analyses avoiding more complicated methodologies such as synchronizing multiple cameras and analyzing multiple video recordings. Our system allowed the performance of the four limbs to be investigated separately without the use of indicators. We also showed that the traditional binary (yes/no) analysis of the faults can be extended by providing qualitatively new information. To date, the few motor performance tasks that are automated (gait analysis, rotarod, parallel rod floor test) only measure one or two aspects of motor behavior (gait, faults, traveled distance). Furthermore, the parallel rod floor test does not provide any information about the faults' origin, parameters, or their spatial distribution.

We tested the recording setup in different groups of mice with different types of motor impairments. In animals with unilateral stroke we showed that various qualities of the foot faults evolve differently with time during the recovery period. For example, long-deep faults showed a transient peak after stroke induction and gradually returned to the pre-stroke levels while short-deep faults remained elevated even 2 months after stroke induction. The combination of neuronal and behavioral compensatory changes might explain the divergent time-dependency of the deep faults. As noted in human stroke patients, compensatory strategies can result in "improvements" in motor performances. The identification of such potential compensatory mechanisms in mice should provide an added advantage when assessing the effectiveness of a certain treatment on stroke recovery (Raghavan, Santello et al., 2010;Takeuchi and Izumi, 2012).

It is interesting to note the lasting presence of shallow foot faults during the recovery period, especially those in the long-shallow category, in contrast to the long–deep faults. The characteristics of the long-shallow foot faults may resemble the human motor neglect syndrome (Plummer, Morris et al., 2003), as these events are typically seen when the animal pushes its snout through a grid hole and the affected forelimb just passively hangs next to it. Our data about the post stroke recovery process show that the novel experimental arrangement is able to resolve details of functional deficits highly resembling those observed in the clinical practice.

In ethanol injected animals we demonstrated that the movement impairment equally affects all four limbs. The number of deep events, particularly the long–deep events showed a robust increase. The appearance of the very long and deep foot faults might be explained by the impaired movement correction and increased reaction time (Hernandez and Vogel-Sprott, 2010; Zoethout, Delgado et al., 2011). We also showed that the moderate dose of ethanol did not alter the locomotor activity but decreased the number of head dippings indicative of exploratory activity, in agreement with previous findings (Lister, 1987; Crabbe, Gallaher et al., 1994). The complex nature of ethanol intoxication and the fact that strains show different behavioral responses to ethanol point to the importance of our approach to evaluate simultaneously various aspects of mouse behavior. This is particularly important when investigating drug effects targeting different aspects of brain function. By providing complex information about several features of the animal's behavior, the use of the method

presented here should decrease the need for consecutive, multiple behavioral tests in the same animal.

Old mice showed different movement disorder patterns: the number of shallow foot faults was dramatically increased. In humans, age related cerebral and cerebellar atrophy (Seidler, Bernard et al., 2010) precipitate the decline in motor performance, and in old mice there is also an age related loss of motor control (Forster, Dubey et al., 1996). These alterations in brain function would lead to an increase in the number of faults. However, other age-related motor function deficits such as the observed slower running speed, shorter distance traveled may have compensatory effects by decreasing the occurrence of more serious deep faults. This also points to the importance of considering multiple parameters when interpreting the results of motor performance tests. It should also be pointed out that the setup provides several other parameters (e.g., speed-fault relation, spatial distribution of the faults) that might provide further details about the characteristics of the movement disability. There is also the possibility of further extending the software to detect other movement related information (e.g., rearing activity from the views in the side mirrors).

5. Conclusions

In summary, we developed a novel video recording arrangement and software to analyze movement deficits in mice. We showed that our new approach was able to provide qualitatively new information about functional motor recovery after stroke. We also showed that it combines several tests to probe for motor and exploratory activity in mice thus simultaneously yielding valuable parameters about various aspects of the activity. Our approach requires no special equipment and therefore it can be implemented by the wider researcher community to many more mouse models of human disorders. In addition, by detecting multiple parameters and combining several tests, our method can significantly lower the number of animals used in research, in agreement with the “replace, refine reduce” goals expressed in a *Nature* editorial (Nature editorials., 2011).

Supplementary Material

Refer to Web version on PubMed Central for supplementary material.

Acknowledgments

This research was supported by an American Heart Foundation Postdoctoral Fellowship to A.M.I.B. and by NIH grants R21NS081438 to I.M., R01AA018316 to Robert Messing (subcontract to I.M.), and the Coelho Endowment to I.M. We are grateful to Reyes Main Lazaro for providing expert assistance with animal care and breeding. The authors declare no conflict of interest.

Reference List

Anderson RM, Shanmuganayagam D, Weindruch R. Caloric restriction and aging: studies in mice and monkeys. Toxicol Pathol. 2009; 37:47–51. [PubMed: 19075044]

Belknap JK. The grid test: A measure of alcohol- and barbiturate-induced behavioral impairment in mice. Behav Res Methods & Instrumen. 1975; 7:66–7.

Boissier JR, Simon P, Lwoff JM. Use of a particular mouse reaction (hole board method) for the study of psychotropic drugs. Therapie. 1964; 19:571–83. [PubMed: 14182942]

Brooks SP, Dunnett SB. Tests to assess motor phenotype in mice: a user’s guide. Nat Rev Neurosci. 2009; 10:519–29. [PubMed: 19513088]

Clarkson AN, Huang BS, Macisaac SE, Mody I, Carmichael ST. Reducing excessive GABA-mediated tonic inhibition promotes functional recovery after stroke. Nature. 2010; 468:305–9. [PubMed: 21048709]

Clarkson AN, Lopez-Valdes HE, Overman JJ, Charles AC, Brennan KC, Thomas CS. Multimodal examination of structural and functional remapping in the mouse photothrombotic stroke model. J Cereb Blood Flow Metab. 2013; 33:716–23. [PubMed: 23385201]

Crabbe JC, Cameron AJ, Munn E, Bunning M, Wahlsten D. Overview of mouse assays of ethanol intoxication. Curr Protoc Neurosci. 2008; Chapter 9(Unit)

Crabbe JC, Gallaher ES, Phillips TJ, Belknap JK. Genetic determinants of sensitivity to ethanol in inbred mice. Behav Neurosci. 1994; 108:186–95. [PubMed: 8192844]

Dombeck DA, Khabbaz AN, Collman F, Adelman TL, Tank DW. Imaging large-scale neural activity with cellular resolution in awake, mobile mice. Neuron. 2007; 56:43–57. [PubMed: 17920014]

Dunham NW, Miya TS. A note on a simple apparatus for detecting neurological deficit in rats and mice. J Am Pharm Assoc Am Pharm Assoc (Baltim). 1957; 46:208–9. [PubMed: 13502156]

Foreman JE, Lionikas A, Lang DH, Gyekis JP, Krishnan M, Sharkey NA, Gerhard GS, Grant MD, Vogler GP, Mack HA, Stout JT, Griffith JW, Lakoski JM, Hofer SM, McClearn GE, Vandenbergh DJ, Blizard DA. Genetic architecture for hole-board behaviors across substantial time intervals in young, middle-aged and old mice. Genes Brain Behav. 2009; 8:714–27. [PubMed: 19671078]

Forster MJ, Dubey A, Dawson KM, Stutts WA, Lal H, Sohal RS. Age-related losses of cognitive function and motor skills in mice are associated with oxidative protein damage in the brain. Proc Natl Acad Sci U S A. 1996; 93:4765–9. [PubMed: 8643477]

Harvey CD, Collman F, Dombeck DA, Tank DW. Intracellular dynamics of hippocampal place cells during virtual navigation. Nature. 2009; 461:941–6. [PubMed: 19829374]

Hernandez OH, Vogel-Sprott M. Alcohol slows the brain potential associated with cognitive reaction time to an omitted stimulus. J Stud Alcohol Drugs. 2010; 71:268–77. [PubMed: 20230725]

Kamens HM, Crabbe JC. The parallel rod floor test: a measure of ataxia in mice. Nat Protoc. 2007; 2:277–81. [PubMed: 17406586]

Leversen JS, Haga M, Sigmundsson H. From children to adults: motor performance across the life-span. PLoS One. 2012; 7:e38830. [PubMed: 22719958]

Lister RG. The effects of ethanol on exploration in DBA/2 and C57Bl/6 mice. Alcohol. 1987; 4:17–9. [PubMed: 3828059]

Metz GA, Whishaw IQ. The ladder rung walking task: a scoring system and its practical application. J Vis Exp. 2009

Metz GA, Whishaw IQ. Cortical and subcortical lesions impair skilled walking in the ladder rung walking test: a new task to evaluate fore- and hindlimb stepping, placing, and co-ordination. J Neurosci Methods. 2002; 115:169–79. [PubMed: 11992668]

Morton SM, Bastian AJ. Cerebellar control of balance and locomotion. Neuroscientist. 2004; 10:247–59. [PubMed: 15155063]

Nature editorials. Animal rights and wrongs. Nature. 2011; 470:435.

Oota S, Mekada K, Fujita Y, Humphries J, Fukami-Kobayashi K, Obata Y, Rowe T, Yoshiki A. Four-dimensional quantitative analysis of the gait of mutant mice using coarse-grained motion capture. Conf Proc IEEE Eng Med Biol Soc. 2009; 2009:5227–30. [PubMed: 19964861]

Plummer P, Morris ME, Dunai J. Assessment of unilateral neglect. Phys Ther. 2003; 83:732–40. [PubMed: 12882614]

Raghavan P, Santello M, Gordon AM, Krakauer JW. Compensatory motor control after stroke: an alternative joint strategy for object-dependent shaping of hand posture. J Neurophysiol. 2010; 103:3034–43. [PubMed: 20457866]

Rozas G, Guerra MJ, Labandeira-Garcia JL. An automated rotarod method for quantitative drug-free evaluation of overall motor deficits in rat models of parkinsonism. Brain Res Brain Res Protoc. 1997; 2:75–84. [PubMed: 9438075]

Schaar KL, Brenneman MM, Savitz SI. Functional assessments in the rodent stroke model. Exp Transl Stroke Med. 2010; 2:13. [PubMed: 20642841]

Seidler RD, Bernard JA, Burutolu TB, Fling BW, Gordon MT, Gwin JT, Kwak Y, Lipps DB. Motor control and aging: links to age-related brain structural, functional, and biochemical effects. Neurosci Biobehav Rev. 2010; 34:721–33. [PubMed: 19850077]

Takeuchi N, Izumi S. Maladaptive plasticity for motor recovery after stroke: mechanisms and approaches. Neural Plast. 2012; 2012:359728. [PubMed: 22792492]

Valenzuela CF, Lindquist B, Zamudio-Bulcock PA. A review of synaptic plasticity at Purkinje neurons with a focus on ethanol-induced cerebellar dysfunction. Int Rev Neurobiol. 2010; 91:339–72. [PubMed: 20813248]

Zoethout RW, Delgado WL, Ippel AE, Dahan A, van Gerven JM. Functional biomarkers for the acute effects of alcohol on the central nervous system in healthy volunteers. Br J Clin Pharmacol. 2011; 71:331–50. [PubMed: 21284693]

Highlights

- Extracting 3D information using single top mounted camera.
- Automated analysis of motor performance of mouse walking on wire mesh.
- Combines multiple behavioral tests: open-field, hole board, grid walking.
- Tested in 3 groups of mice with different neurological deficits.

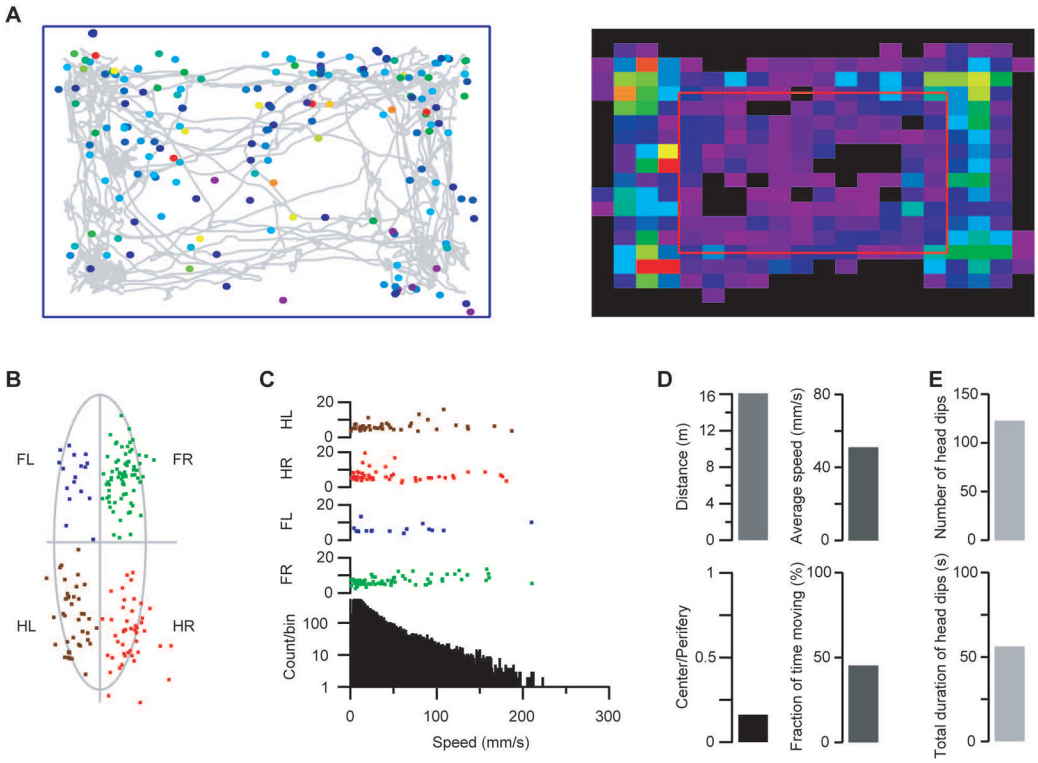

Figure 1.

The various movement characteristics calculated by the software. A) *Left*: Animal trajectory during the recording (grey line). Colored circles indicate the foot fault locations (from purple to red: depth of fault). *Right*: Location preference. Cell colors indicate the normalized time spent in the respective cell (from purple to red: longer time). Red rectangle separates the center and periphery of the grid matrix. B) Sample relative fault locations in a mouse with a stroke in the left motor cortical forelimb area. Note the prominent increase in the number of faults by the right forelimb. The mouse's body was approximated by an ellipsoid in a frame-by-frame manner. If a fault occurred the relative fault coordinates were calculated as the fraction of major axis vs the fraction of minor axis from the center of the corresponding ellipsoid. Different colors indicate the origin of the fault origin (*green*: right forelimb, FR; *blue*: left forelimb, FL; *red*: right hind limb, HR; *brown*: left hind limb, HL). C) Instantaneous speed of movement on the grid and fault occurrence in the same animal. *Bottom*: instantaneous speed histogram. *Top four rows*: fault depth and instantaneous speed at time of occurrence on each limb. D) *Top left*: total distance traveled by the animal during the recording. *Top right*: average speed during movement. *Bottom left*: ratio of the time spent in the center vs periphery (as indicated in *A*). *Bottom right*: fraction of time spent moving. D) Exploration on the grid used as a holeboard: *top*: number of head dips; *bottom*: total duration of head dips.

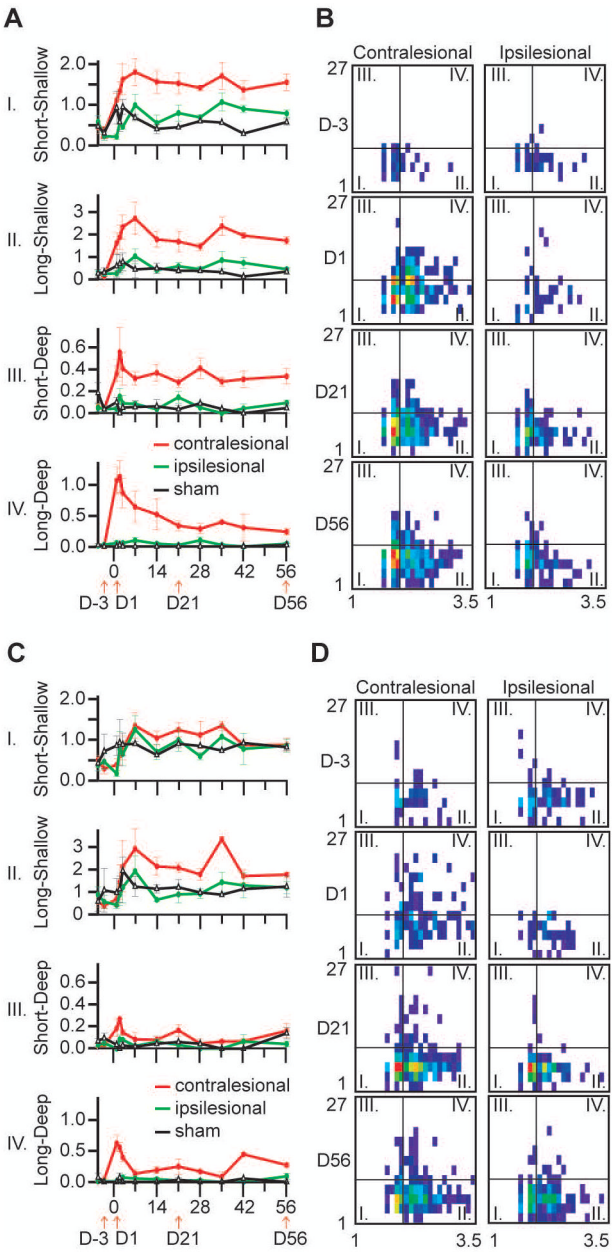

Figure 2.

Time course of foot faults after stroke induction. A) Number of forelimb faults with different characteristics (duration and depth) normalized to the traveled distance at various timepoints before and after stroke induction in the forelimb motor cortex (red: contralesional forelimb; green: ipsilesional forelimb; black: sham control). Note the differential evolution of the number of faults after stroke induction; the deep events are nearly absent from the sham or prestroke animals. B) Averaged and distance normalized duration-depth matrices at certain timepoints before and after stroke induction: each cell of the 2D histograms shows the normalized number of faults (color scaled) with the corresponding duration (horizontal axis) and depth (vertical axis) values. The timepoints indicated at the middle of each row are corresponding to the timepoints indicated by arrows in *A*). The thin vertical and horizontal lines on each matrix indicate the defined borders between the short-long and shallow-deep

faults. Roman numerals in the matrices indicate the fault quadrants and correspond to the diagrams in *a*) labeled with the same roman numerals. The horizontal axis of the matrices show the fault duration (log scale), the vertical axes show the depth in pixels. C) and D) same animals and arrangement as in A) and B) but showing the hind limb faults. Note that the hind limbs are less affected since the stroke was targeted at the forelimb motor cortical area. (traces show mean ± s.e.m, *n=4* stroked animals, *n=2* sham control animals).

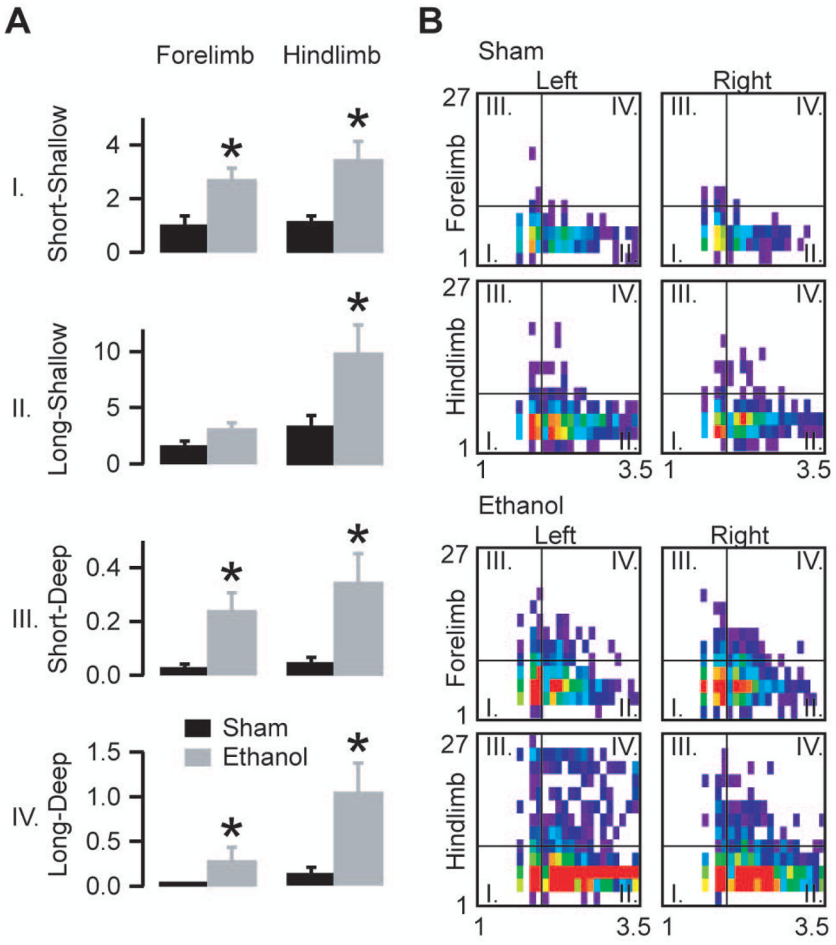

Figure 3.

Movement characteristics after a moderate dose of ethanol. A) Average normalized fault numbers in the quadrants of the duration-depth matrices. B) Averaged and distance normalized duration-depth matrices for the four limbs divided into four quadrants as indicated in the legend of Fig 2B. Note the appearance after ethanol administration of very long faults, especially on the hind limbs. The horizontal axes of the matrices denote fault duration (log scale), the vertical axes indicate depth in pixels (asterisks mark statistically significant differences $p<0.05$; bars show mean ± s.e.m, $n=8$ ethanol injected animals, $n=8$ saline injected animals; unpaired two-tailed t-test, forelimb short-shallow $p=0.007$; forelimb long-shallow $p=0.1$; forelimb short-deep $p=0.008$; forelimb long-deep $p=0.02$; hind limb short-shallow $p=0.009$; hind limb long-shallow $p=0.03$; hind limb short-deep $p=0.02$; hind limb long-deep $p=0.01$).

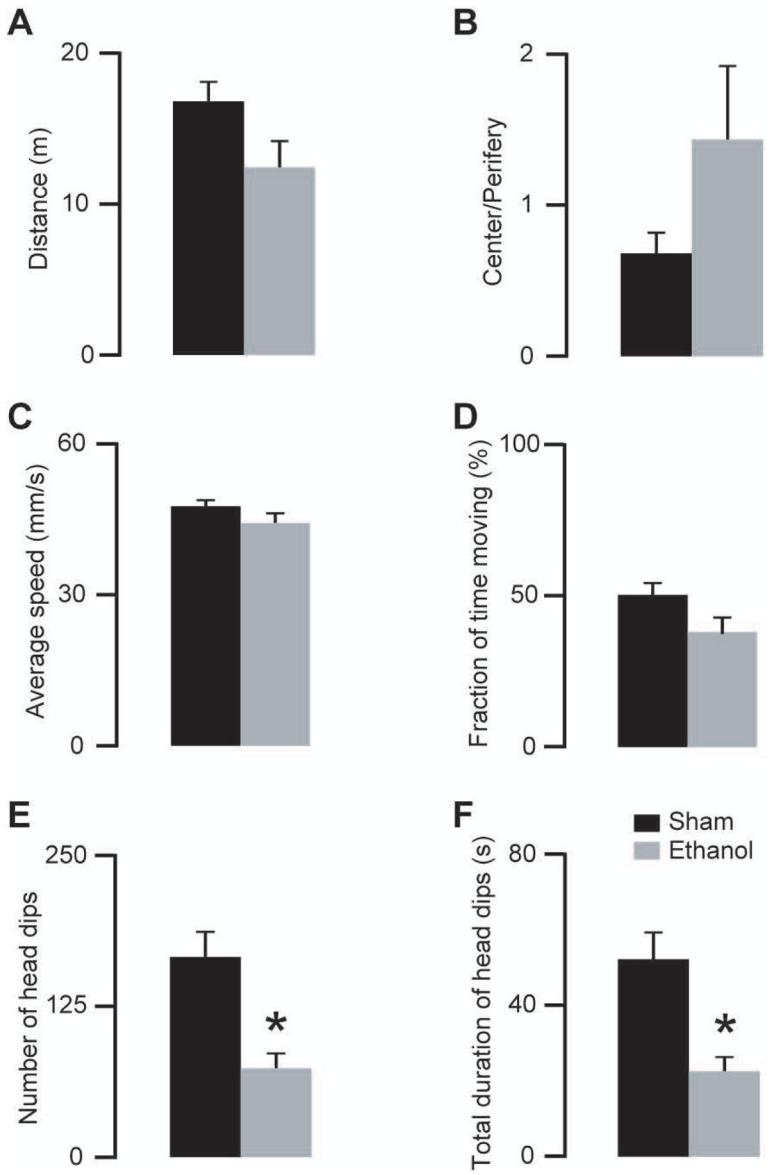

Figure 4.

Effects of a moderate dose of ethanol (1.6 g/kg i.p.) on locomotor and exploratory activities. A–D) Ethanol (*grey bars*) did not change the locomotor activity of the mice compared with saline injected (*black bars*) mice (unpaired two-tailed t-test, $p>0.07$ for all comparisons). E–F) Ethanol treated animals showed less head dips (unpaired two-tailed t-test, $p=0.003$) and decreased duration of the total head dips (unpaired two-tailed t-test, $p=0.004$) (*indicate statistically significant differences $p<0.05$; $n=8$ ethanol, $n=8$ saline injected mice, same animals as on Fig 3).

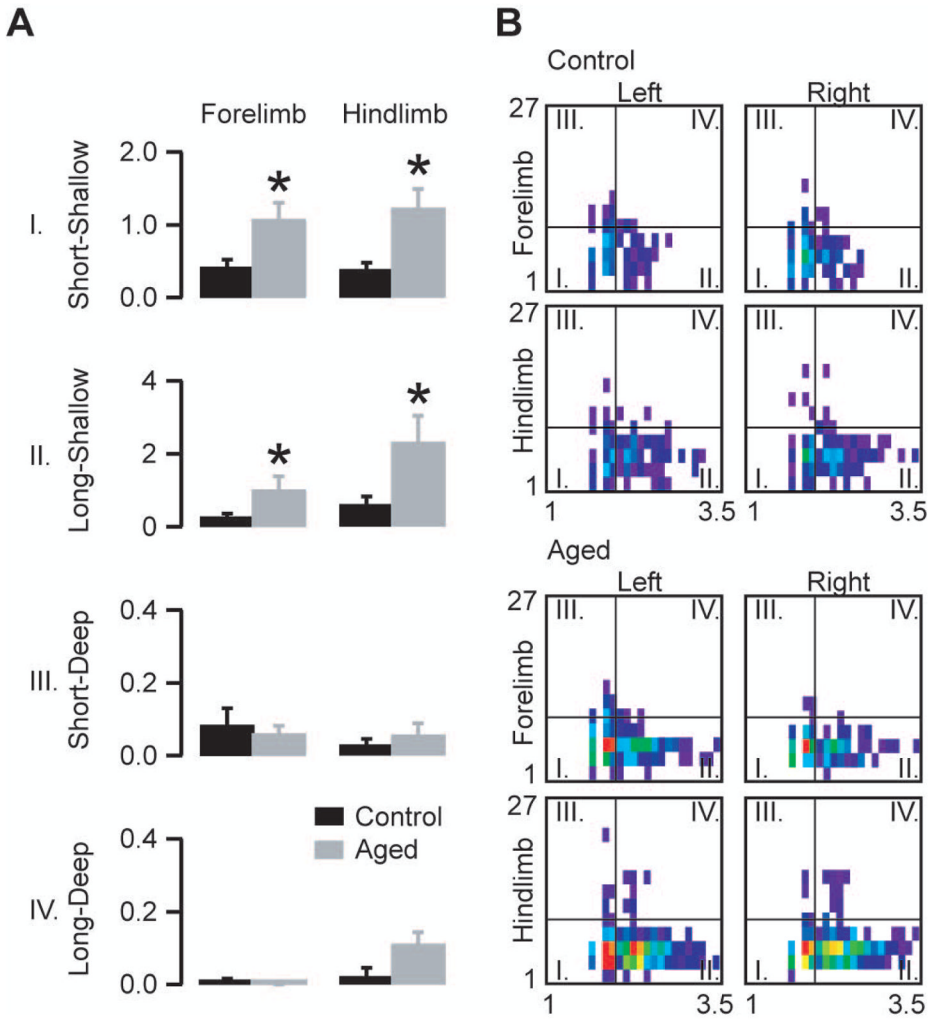

Figure 5.

Fault characteristics in aged (96–99 weeks old) mice compared to young adult (8–12 weeks old) mice. A) Average normalized fault numbers in the quadrants of the duration depth matrices. B) Averaged and distance normalized duration-depth matrices for the four limbs divided into four quadrants as indicated in the legend of Fig 2B. Note that the most prominent differences between old and young adult mice are in the numbers of shallow events. The horizontal axes of the matrices denote fault duration (log scale), the vertical axes indicate depth in pixels (asterisks mark statistically significant differences, unpaired two-tailed t-test, $p<0.05$; bars show mean ± s.e.m, $n=6$ aged animals, $n=6$ young adult animals; forelimb short-shallow $p=0.01$; forelimb long-shallow $p=0.04$; forelimb short-deep $p=0.6$; forelimb long-deep $p=0.3$; hind limb short-shallow $p=0.005$; hind limb long-shallow $p=0.03$; hind limb short-deep $p=0.3$; hind limb long-deep $p=0.06$)

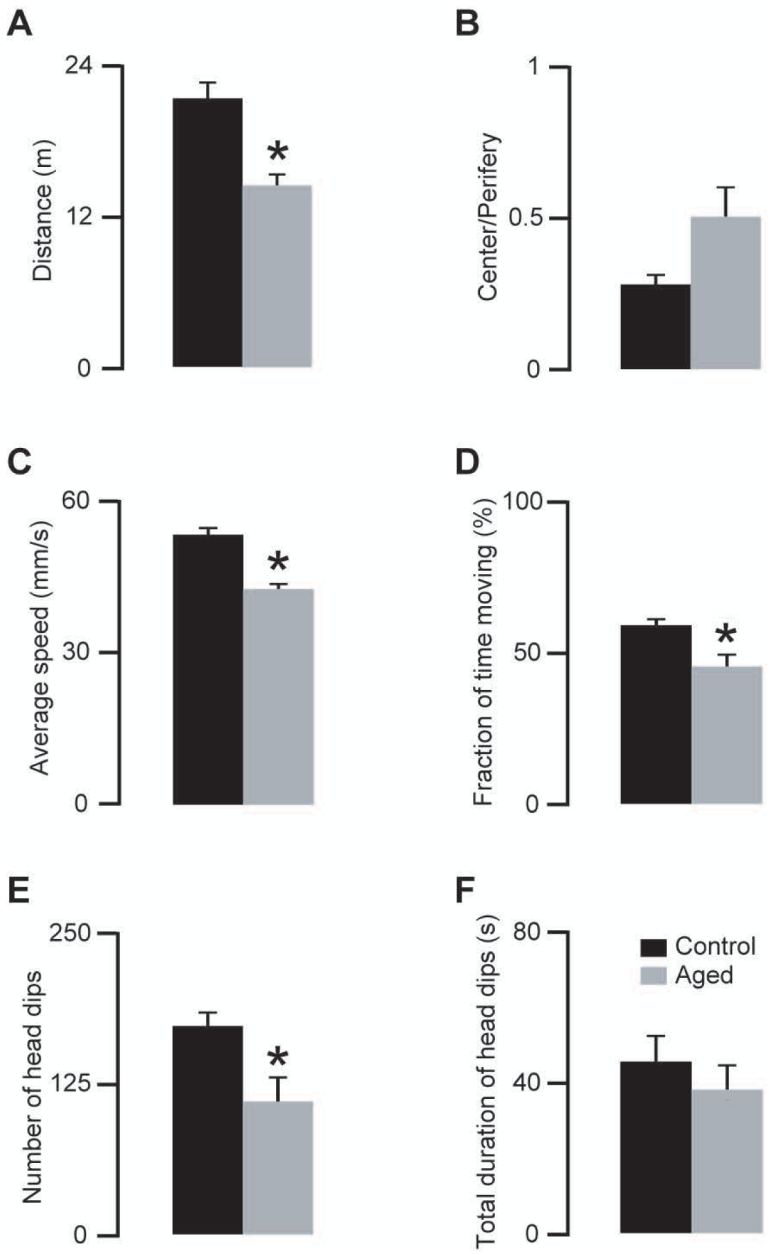

Figure 6.

Effects of ageing on locomotor and exploratory activities. A–D) Aged (96–99 weeks old) mice showed decreased locomotor activity compared with young adult (8–12 weeks old) mice (comparisons, traveled distance, unpaired two-tailed t-test, p=0.001; center/periphery, unpaired two-tailed t-test, p=0.06; average speed, unpaired two-tailed t-test, p=0.0001; fraction of time moving, unpaired two-tailed t-test, p=0.01). E–F) The same aged animals showed less head dips (unpaired two-tailed t-test, p=0.02), however the total duration of the head dips did not change significantly (unpaired two-tailed t-test, p=0.4) (* indicate statistically significant differences p<0.05, n=6 aged, n=6 young adult mice; same animals as on Fig 5).